Star-Planet Interactions: Planet evaporation around low-mass stars

SUVRAT RAO
5th -year Physics student
IIT Kharagpur
Student ID: 14PH20027

Guide: Prof. GEORGES MEYNET
Head, Stellar Evolution Group
Geneva Observatory, Switzerland

I. INTRODUCTION

We study the time evolution of a star-planet system consisting of a single planet in a circular orbit around its host star, taking into account the evolution of the internal structure of the star, the spin of the star, the stellar mass-loss and magnetic braking due to stellar winds, tidal interactions (equilibrium and dynamical tides in stellar convective zones), mass/radius change of the planet (accretion and evaporation), drag experienced by the planet (frictional and gravitational), and the secular evolution of the planetary orbit. It is assumed that at the beginning of the time-evolution, the proto-planetary disk has fully dissipated, planet formation is complete, and the proto-star has just entered its Pre-Main Sequence (PMS) phase.

In this study, the host star is a 1 Solar-mass star at solar metallicity (equivalent to the Sun). Two cases are considered for the stellar spin: a fast-rotating versus a slow-rotating star. We consider close-in planets, with the initial orbital distance being of the order ~ 0.01 au since this is the domain where the star-planet interactions have a significant effect on the planet. Regarding the planet mass, beyond a few Jupiter masses, the star-planet interactions can also begin to significantly affect the stellar spin (such effects will be studied in future works), so we restrict our study to planetary masses from 0.0 up to a few Jupiter masses. The time-evolution of the system is carried out, in terms of the phases of stellar evolution, from the start of the Pre-Main Sequence (PMS) phase up to the beginning of the Red Giant Branch (RGB) phase. For a solar-like star, this entails a timescale of ~10 Gyrs.

The results of this study are numerically obtained by computing the time-evolution of the star-planet system using a computer code. The assumption we use in our model to increase computational efficiency is that the evolution of the internal structure of a star is independent of the presence of a planet i.e. star-planet interactions only affect the *spin* of the star. Hence, we can use the internal structure evolution data of an isolated star (from the output of a stellar evolution code, in this case, the **Geneva Code**) and introduce the planet as a perturbation, calculating the stellar spin simultaneously with the evolution of the planet. This assumption is especially valid in the domain of this study, where the star-planet interactions have a significant effect only on the planet, and not on the star.

In a previous work, titled 'Star-planet interactions. V. Dynamical and equilibrium tides in convective zones' (Rao et al. 2018), we studied specifically the impact of star-planet interactions (tides) on the orbital evolution and possible engulfment of planets by the host star. In the results of this study, we focus mainly on the mass-loss (evaporation) of the planets and discuss some implications of planet engulfment and evaporation for observational astronomy. Since the physics of stars and planets is still not completely known and new discoveries are being made every day, it is fruitful to focus on some definite, robust and reliable *qualitative* trends which can be used to guide observations. The observations can in turn constrain the parameters of our models and improve our understanding of the physics of stars and planets.

This study shall be repeated in a similar manner for other types of low-mass stars (1.5 Solar-mass star) before the results are published in a sequel paper to the previous one.

II. MODEL DESCRIPTION

Stellar Physics:

Stellar internal structure evolution: This is computed via the *Geneva Stellar Evolution Code* for an isolated star of given mass, metallicity and initial spin. The internal structure corresponds to variables like the stellar radius, mass, temperature, luminosity, composition (mass fractions of elements), the mass and size of the convective and radiative zones etc. The output files of the Geneva Code are used as the input for our star-planet system evolution code.

Stellar spin evolution: For calculating the stellar spin, the interior of the star is divided into two separate homogenous regions (for a solar-like star, they are the 'radiative core' and the 'convective envelope'). This corresponds to the homogenous, piecewise 2-layer model given by MacGregor and Allain (1991, 1998). The radiative core and convective envelope can undergo differential rotation, and the sizes of these regions change as the star evolves in time. Due to this, there is an exchange of angular momentum between these two zones, termed 'core-envelope coupling'. The first contribution to the coupling is due to differential rotation, and the second contribution is due to the changing size of the zones with time (some region of the convective zone becomes a part of the radiative zone as the star progresses from the PMS to the MS and the vice versa during the RGB phase). The rate of angular momentum exchange due to differential rotation is calculated by finding the maximum possible exchange of angular momentum between the two differentially rotating regions (by conserving angular momentum between the initial state and a final state where there is no differential rotation) and dividing it by a coupling timescale which is empirically obtained for different star-types.

Apart from the core-envelope coupling, the convective envelope exclusively has two more contributions to its net rate of change of angular momentum. The first of these is due to magnetic braking by the stellar winds. The charged stellar wind particles are boosted by the magnetic field of the star (which arises because of the stellar dynamo). This causes an equal

and opposite Lorentz force to act on the star which brakes (slows down) its spin over time. We use the wind-braking prescription given by Matt et al. (2012). The second contribution to the net rate of change of the convective envelope angular momentum is due to the star-planet interactions (tides in the stellar convective zone), which cause an exchange of angular momentum between the star and the planet. This term can be obtained by taking the negative time derivative of the planet's angular momentum and neglecting any dissipative terms (which only affect the planet), keeping only the tidal term (which causes an equal and opposite exchange of angular momentum between the star and planet).

Overall, the equations describing the spin evolution of the star are as follows:

$$\dot{L}_{envelope} = \dot{L}_{wind-braking} + \dot{L}_{core-envelope-coupling} + \dot{L}_{star-planet-\mathrm{interactions}}$$

$$\dot{L}_{core} = -\dot{L}_{core-envelope-coupling}$$

$$\dot{L}_{wind-braking} = -\frac{2}{3}(K_1 K_3)^2 M_{star}^{(1-2m)} R_{star}^{(2+4m)} B_0^{4m} \frac{\omega_{envelope}}{\left(K_2^2 v_{esc}^2 + \omega_{envelope}^2 R_{star}^2\right)^m}$$ -- Matt et al. (2012)

$$\dot{L}_{core-envelope-coupling} = \frac{\Delta J_{\max}}{t_{coupling}} - \frac{2}{3} R_{core}^2 \omega_{envelope} \dot{M}_{core}$$ -- MacGregor and Allain (1991, 1998)

$$\dot{L}_{star-planet-interactions} = -\left[\frac{1}{2} m_{planet} \left(\frac{\dot{a}}{a}\right)_{tides}\right] . \sqrt{G(M_{star} + m_{planet})a}$$

K_1=1.3, K_2=0.0506, K_3=1, m=0.2177 as given by Matt et al. (2012). B_0 is the stellar magnetic field, which is calculated as in See et al. (2017), who have found that B_0 scales as a power law function of the Rossby number (ratio of the stellar rotation timescale to the convective timescale). v_{esc} is the escape velocity at the stellar surface. We use a coupling timescale prescription as given by Spada et al. (2011).

Stellar Winds: We use the Isothermal Coronal Wind model (Parker, 1958) for the stellar wind prescription. Stellar winds result in mass-loss by the star, magnetic-braking of the stellar convective envelope, and contribution to the Inter-Planetary Medium (IPM) density, leading to drag and mass-accretion by the planet. More sophisticated stellar wind models exist than the one used here. We choose this model over others due to the following reasons:

- Wind velocity, density and mass-loss expressions are analytical, making the implementation of the model computationally less expensive.
- This model is known to be accurate for low-mass stars up to ~5 au (our domain of close-in planets is therefore well within this range).
- Other wind models are very specific to star-types whereas this model is a little general, making our code versatile.

- High accuracy of the stellar wind model is not necessary, since it only affects planet drag and mass accretion, which are less significant compared to tides and mass evaporation. Also, as long as the stellar mass-loss rate is of the correct order, the wind model does not sensitively affect magnetic wind braking.

The wind velocity profile, density profile and stellar mass-loss rate are given by the following expressions:

$$\left(\frac{v_{wind}}{v_s}\right)^2 .e^{-\left(\frac{v_{wind}}{v_s}\right)^2} = \left(\frac{r_s}{r}\right)^4 .e^{-4\left(\frac{r_s}{r}\right)+3}$$

$$\rho_{wind} = \frac{\rho_1 . v_1}{r^2 . v_{wind}}$$

$$\dot{m}_{winds} = -\left|4\pi R_{star}^2 \rho_1 v_1\right|$$

v_s is the speed of sound in the medium, r is the distance from the center of the star in units of stellar radii, r_s is the sonic distance (where the wind velocity becomes equal to v_s). ρ_1 and v_1 are the wind density and velocity at the stellar surface (photosphere).

Planetary Physics:

Planet Structure: We assume a spherical planet of uniform density. Because of planet formation processes, we expect a planet with a specified mass to have a definite radius which is a function of its mass (there may be a spread in this value depending on the composition of the planet). Therefore, we use a mass-radius relation to calculate the initial radius of a planet of given mass. We use the prescription given by Bashi, Helled, Zucker and Mordasini (2017), which is a piece-wise power law relation between planet mass and radius obtained by using advanced statistical techniques to fit the power law with direct observational exoplanet data and with numerical simulations of planet formation. The piece-wise description provides a distinction between 'small' and 'large' planets :

$$r_{planet} = r_t \left(\frac{m_{planet}}{m_t}\right)^{0.55} \quad \text{if } m_{planet} < m_t$$

$$r_{planet} = r_t \left(\frac{m_{planet}}{m_t}\right)^{0.01} \quad \text{if } m_{planet} >= m_t$$

The transition mass separating the 'small' planets from the 'large' planets is $m_t = 124.0 * m_{Earth}$ and the transition radius is $r_t = 12.1 * r_{Earth}$.

We ascribe to the planets a magnetic field, which planets usually possess, and which plays a role in the drag and mass-accretion experienced by the planet. However, we do not consider any interactions between the stellar and planetary magnetic fields. Since planetary magnetic fields arise because of a planetary dynamo, and since these processes are not yet well known (and difficult to model), we use a simple prescription – small planets are assigned Earth's magnetic field and large planets are assigned Jupiter's magnetic field. The distinction between 'small' and 'large' planets is, as before, made using the piecewise mass-radius relation.

Planet Orbital Evolution: The secular evolution of the planetary orbit is governed by three processes – Firstly, the planet experiences drag whilst traversing through the inter-planetary medium (IPM). The drag has two contributions viz. frictional and gravitational. Frictional drag on the planet is due to the form-drag experienced by a sphere moving through a fluid. As the planet moves through the IPM, it may displace, accrete and disrupt the medium, leaving behind a wake which creates a non-uniformity in the IPM. This in turn exerts a gravitational pull on the planet, which acts as gravitational drag.

The second process is equivalent to a thrust force, which is caused by changing planetary mass. The planet can accrete mass onto itself from the IPM or it may lose mass through evaporation due to strong XUV irradiation from the star. The star also continuously loses mass due to stellar winds. Since the star-planet system is a binary system, a net mass-change in the system will result in a thrust force which will change the orbital distance.

Finally, the most important process that governs the orbital secular evolution is the star-planet interactions, i.e. gravitational tides. Tides act on both the star and the planet. In the star, tides can act in different regions (convective zone or radiative zone). We neglect planetary tides here, since we do not have a detailed prescription for the internal structure of the planet and because planetary tides will affect the rotation of the planet, which we do not care about in this study. We consider tides which take place in the stellar convective zone. The complete tidal prescription in stellar convective zones is two-fold – The first type of tides is called 'Equilibrium Tides', which arise because of the deformation in any celestial body caused by the non-uniform gravitation applied by its companion to different parts of the extended body. This deformation rotates about the body's axis because the gravitating companion orbits the body. If all processes are perfectly elastic, the deformation always points along the two-body axis and no tides occur. But equilibrium tides can get dissipated in the convective envelope of stars due to turbulence. Hence, there is an offset between the rotation of the deformation and the orbiting companion. The companion's gravitational pull on the deformation can therefore apply a torque on the body, thus leading equilibrium tides to cause an exchange of angular momentum between the star and planet. The complete description of tides in convective zones, however, involves a second type of tides called 'Dynamical Tides', which arise because the orbiting gravitating companion can induce inertial waves inside the body, whose restoring force is the Coriolis force. Dynamical tides also cause an exchange of angular momentum between the star and planet.

It is found that Equilibrium tides are the dominant tides during the RGB phase of the star, while Dynamical tides are dominant during the PMS phase (Rao et al. 2018). Note that both

tides occur in the convective region of the star and are active only in those stages of the stellar evolution where the star has a large convective region. The effect of both the tides is to shrink the orbital distance if it is less than the corotation radius (the distance at which the planet orbital spin equals the stellar spin) or expand the orbital distance if it is greater than the corotation radius. There are no tides if the orbital distance is equal to the corotation radius.

We implement the orbital evolution prescription as used in Rao et al. (2018). The equations governing the orbital secular evolution are given as follows:

$$\left(\frac{\dot{a}}{a}\right)_{net} = \left(\frac{\dot{a}}{a}\right)_{drag} + \left(\frac{\dot{a}}{a}\right)_{mass-change} + \left(\frac{\dot{a}}{a}\right)_{tides}$$

$$\left(\frac{\dot{a}}{a}\right)_{drag} = -\frac{2}{M_{pl}v_{pl}}\left[\frac{1}{2}C_d\rho_{wind}v_{pl}.2\pi r_{pl\_eff}^2 + 4\pi\left(\frac{GM_{pl}}{v_s}\right)^2\rho_{wind}I\right]$$

$$\left(\frac{\dot{a}}{a}\right)_{mass-change} = -\frac{\dot{M}_{star} + \dot{M}_{pl}}{M_{star} + M_{pl}}$$

$$\left(\frac{\dot{a}}{a}\right)_{eq-tides} = \frac{f}{\tau}\frac{M_{env}}{M_{star}}\frac{M_{pl}}{M_{star}}\left(1 + \frac{M_{pl}}{M_{star}}\right)\left(\frac{R_{star}}{a}\right)^8\left(\frac{\omega_{star}}{\omega_{pl}} - 1\right)$$

$$\left(\frac{\dot{a}}{a}\right)_{dyn-tides} = \left(\frac{9}{2Q_d'}\right)\frac{M_{pl}}{M_{star}}\omega_{pl}\left(\frac{R_{star}}{a}\right)^5 \mathrm{sgn}(\omega_{star} - \omega_{pl})$$

The subscript 'pl' corresponds to 'planet'. C_d =0.9 is the drag coefficient of a sphere. r_{pl_eff} is the effective planetary radius for the frictional drag and it may be greater than the actual planetary radius due to the planet's magnetic field, which can contribute to the frictional drag by interacting with charged particles in the IPM. 'I' is a function of the Mach number which can be taken to have a constant value of 0.5.'f' is a numerical factor which depends on the Rossby number and τ is the convective timescale. Q'_d is the quality factor for dynamical tides and it is a function of the internal structure parameters of the star (Ogilvie 2013; Mathis 2015). The attractive or repulsive behaviour of the tides described earlier is contained in the sign of the $(\omega_{star} - \omega_{pl})$ terms.

Note: The Dynamical tidal prescription used here is a frequency averaged formula, and the condition for the dynamical tides to be active is that $\omega_{pl} < 2\omega_{envelope}$. Also, the equilibrium and dynamical tides are active only if a convective region is present in the star.

Planet Mass and Radius change: The planet may gain mass from accreting the IPM material onto itself or may lose mass because of evaporation due to strong XUV irradiation by the star. The radius change is directly related to the mass change and can be written as :

$$\dot{R}_{pl} = \frac{1}{3}\frac{\dot{M}_{pl}}{M_{pl}} R_{pl}$$

We use the mass-accretion prescription given by Bondi & Hoyle (1944) and the density of the IPM is obtained from our stellar wind model (the IPM is formed mostly from the material lost by the star via stellar winds). For the mass-evaporation process, we use the prescription as mentioned in Lalitha et al. (2018):

$$\dot{M}_{pl-net} = |\dot{M}_{pl-accr}| - |\dot{M}_{pl-evap}|$$

$$R_{accr} = \frac{2GM_{pl}}{v_{pl}^2}$$

$$\dot{M}_{pl-accr} = \pi R_{accr}^2 \rho_{wind} v_{pl}$$ -- Bondi & Hoyle (1944)

$$\dot{M}_{pl-evap} = \frac{3\pi}{4}\frac{\varepsilon\beta^2}{\kappa}\frac{F_{XUV}}{G\rho_{pl}}$$ -- Lalitha et al. (2018)

R_{accr} is the Bondi accretion radius. F_{XUV} is the radiation flux emitted by the star corresponding to the X-ray and UV regime of the EMR, which is known to be the cause of material evaporation from both rocky and gaseous planets. It consists of two contributions – The first is the thermal contribution due to the black-body radiation of the star which can be calculated knowing the total flux, by multiplying it with a factor which is a Bose-Einstein integral that comes from integrating the Planck black-body radiation law in the XUV regime. The second is a non-thermal contribution. The non-thermal XUV flux arises due to the radiation emitted by the charged stellar-wind particles which get boosted by the star's magnetic field. The X-ray contribution scales as a power law function of the Rossby number given by Tu, Johnstone, Güdel, and Lammer (2015). The UV contribution can be obtained via an empirical relation between the UV and the X-ray contributions. 'ε' is a factor that takes care of the planet composition, and the value ε =0.4 can be used for both hot-Jupiters as well as strongly irradiated rocky planets (Valencia et al. , 2010). 'κ' is a factor which takes care of mass loss due to Roche-lobe overflow. 'β' is a correction factor that handles the effective size of the planet absorbing the incident XUV radiation.

III. NUMERICAL METHODS

From the previous section, we see that overall, we have a system of coupled ODEs :

$$\dot{a} = f(a, \dot{a}, R_{pl}, \dot{R}_{pl}, M_{pl}, \dot{M}_{pl}, L_{env}, \dot{L}_{env}, L_{core}, \dot{L}_{core}, \dots)$$
$$\dot{M}_{pl} = g(a, \dot{a}, R_{pl}, \dot{R}_{pl}, M_{pl}, \dot{M}_{pl}, L_{env}, \dot{L}_{env}, L_{core}, \dot{L}_{core}, \dots)$$
$$\dot{R}_{pl} = h(a, \dot{a}, R_{pl}, \dot{R}_{pl}, M_{pl}, \dot{M}_{pl}, L_{env}, \dot{L}_{env}, L_{core}, \dot{L}_{core}, \dots)$$
$$\dot{L}_{env} = u(a, \dot{a}, R_{pl}, \dot{R}_{pl}, M_{pl}, \dot{M}_{pl}, L_{env}, \dot{L}_{env}, L_{core}, \dot{L}_{core}, \dots)$$
$$\dot{L}_{core} = v(a, \dot{a}, R_{pl}, \dot{R}_{pl}, M_{pl}, \dot{M}_{pl}, L_{env}, \dot{L}_{env}, L_{core}, \dot{L}_{core}, \dots)$$

Also, we note that 'time' does not explicitly occur in any of the coupled ODEs. Hence, for this situation, an efficient technique for numerical computations is the *Runge-Kutta 4th order method for a system of coupled ODEs.*

Since the distance, mass and time-scales in astronomy are very large (~0.01 au, ~1MJu and ~10Gyr respectively in our case), and since we are interested in deriving some definite, reliable and robust *qualitative* trends from the results, we are not concerned with any error tolerance as is usually calculated in any numerical integration technique.

IV. RESULTS

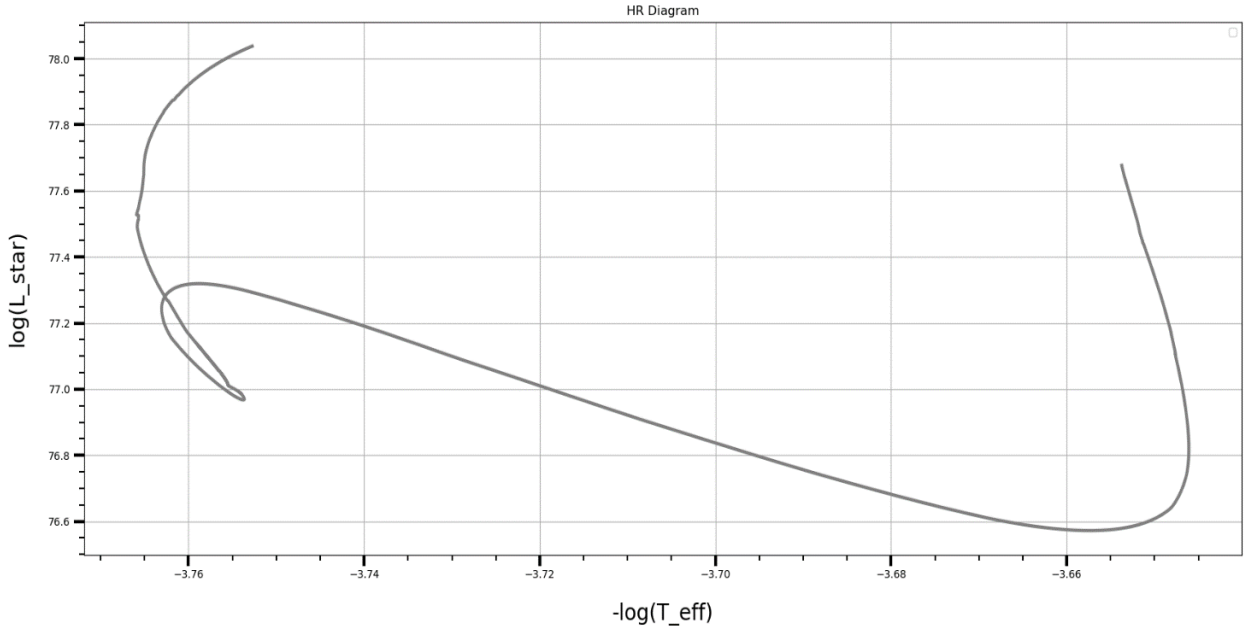

Fig. 1 – HR diagram of a 1M_Sol star (from PMS up to the beginning of RGB phase)

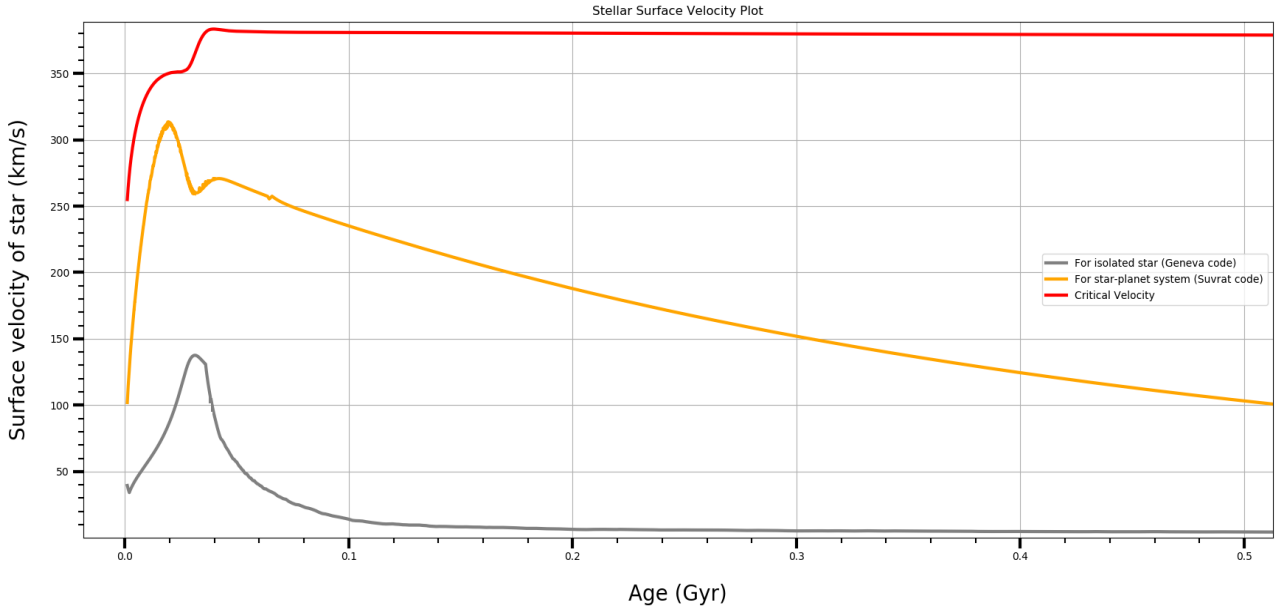

Fig. 2 – Stellar surface-velocity evolution (slow vs. fast rotating 1M_Sol star)

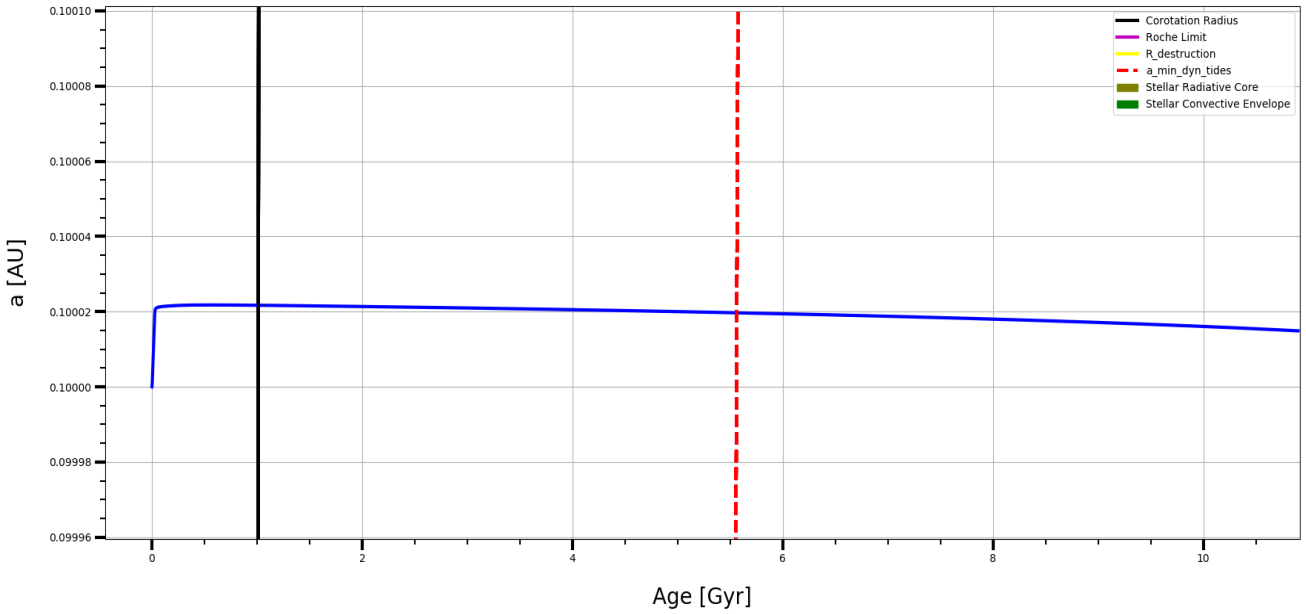

Fig. 3.1 – Orbital evolution of a 30*M_Earth planet initially at 0.1 au around a slow-rotating 1M_Sol star showing the effect of dynamical tides during the PMS and slow orbital decay due to drag.

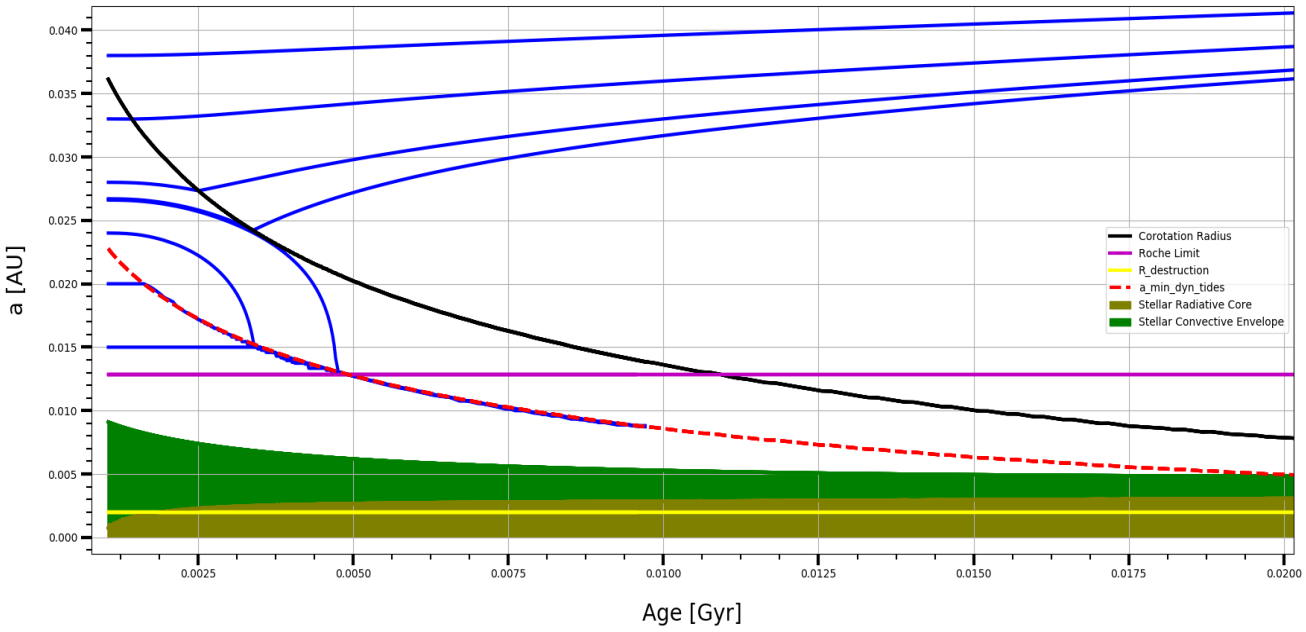

Fig. 3.2 – Orbital evolution of a close-in 30*M_Earth planet around a slow-rotating 1M_Sol star showing the effect of dynamical tides during the PMS.

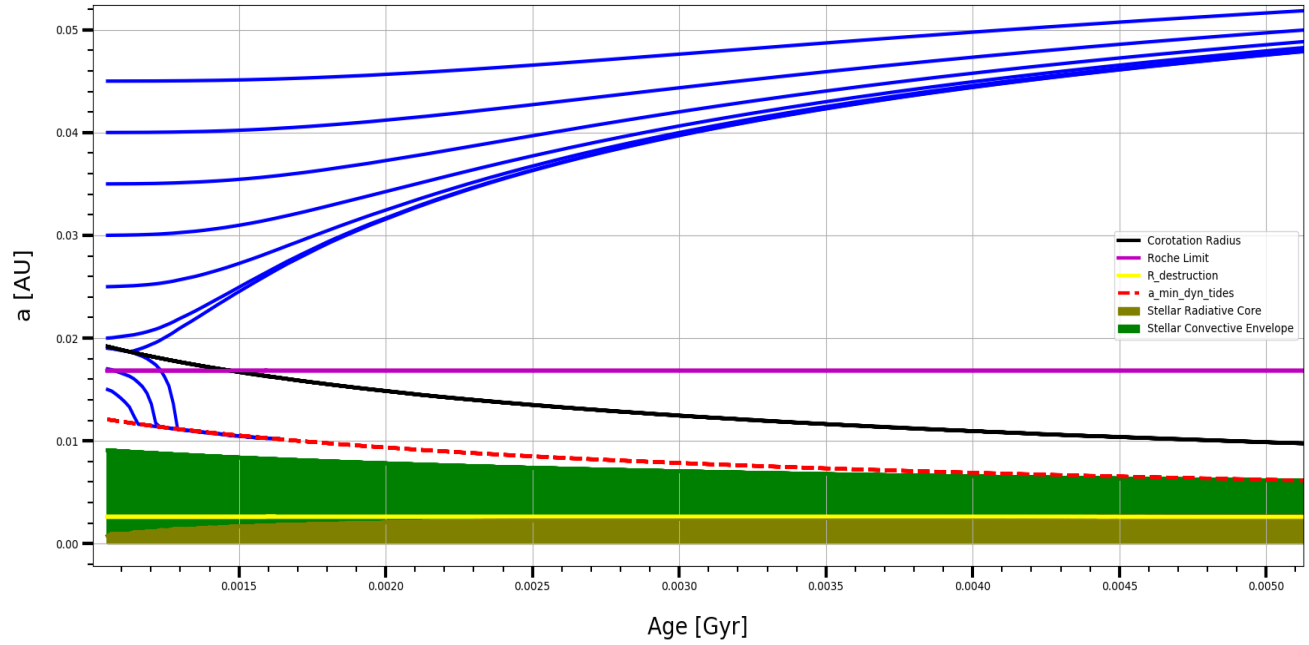

Fig. 3.3 – Orbital evolution of a close-in 140*M_Earth planet around a fast-rotating 1M_Sol star showing the effect of dynamical tides during the PMS.

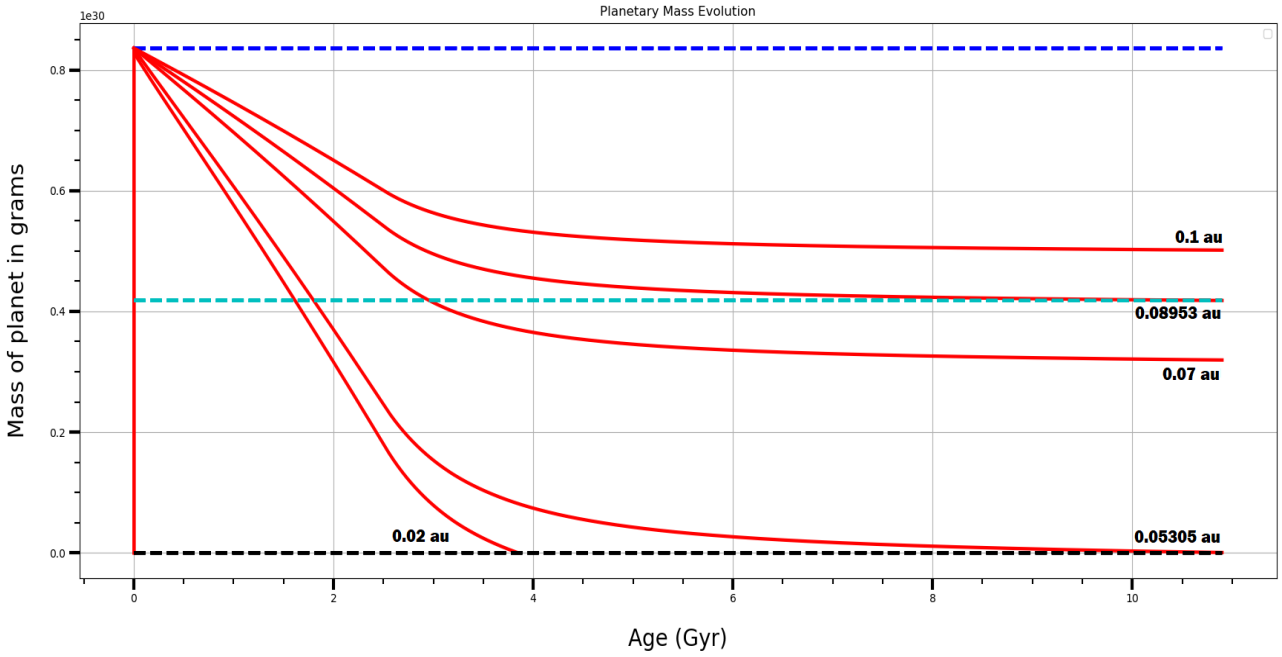

Fig. 4.1 – Mass evolution of a close-in 140*M_Earth planet around a fast-rotating 1M_Sol star at different initial distances (from PMS up to the beginning of RGB phase).

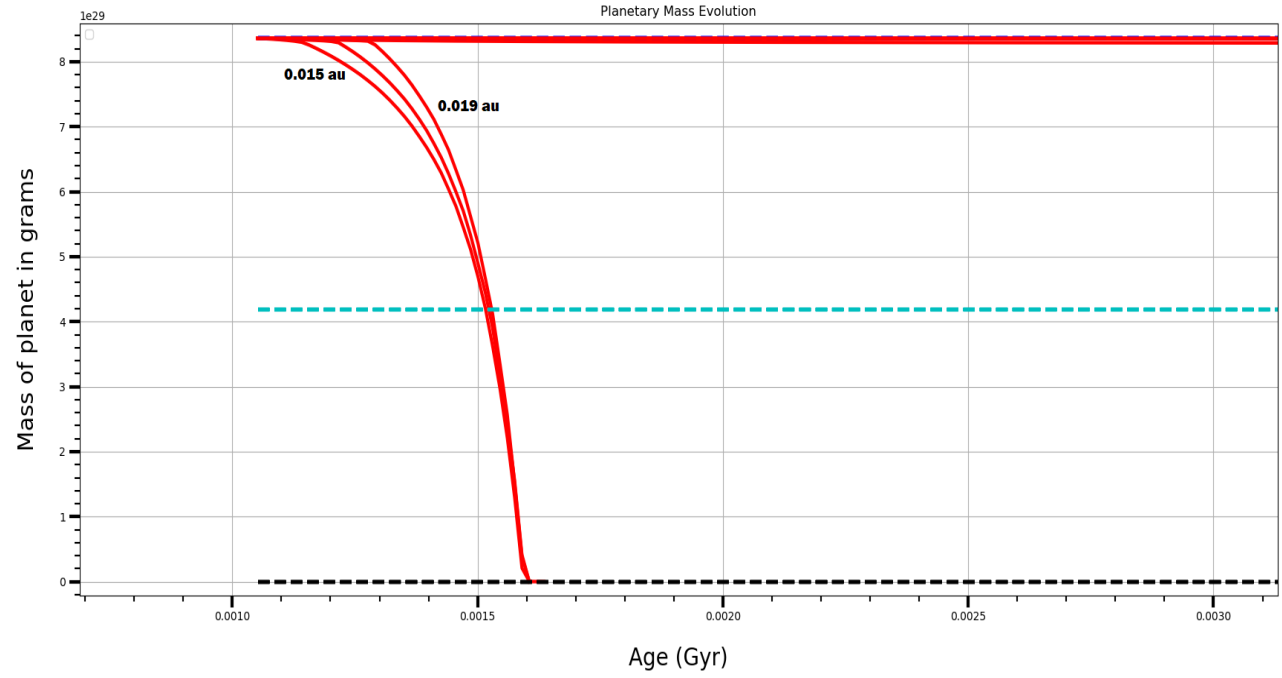

Fig. 4.2 – Zoom-in on the left-most curve in Fig. 4.1

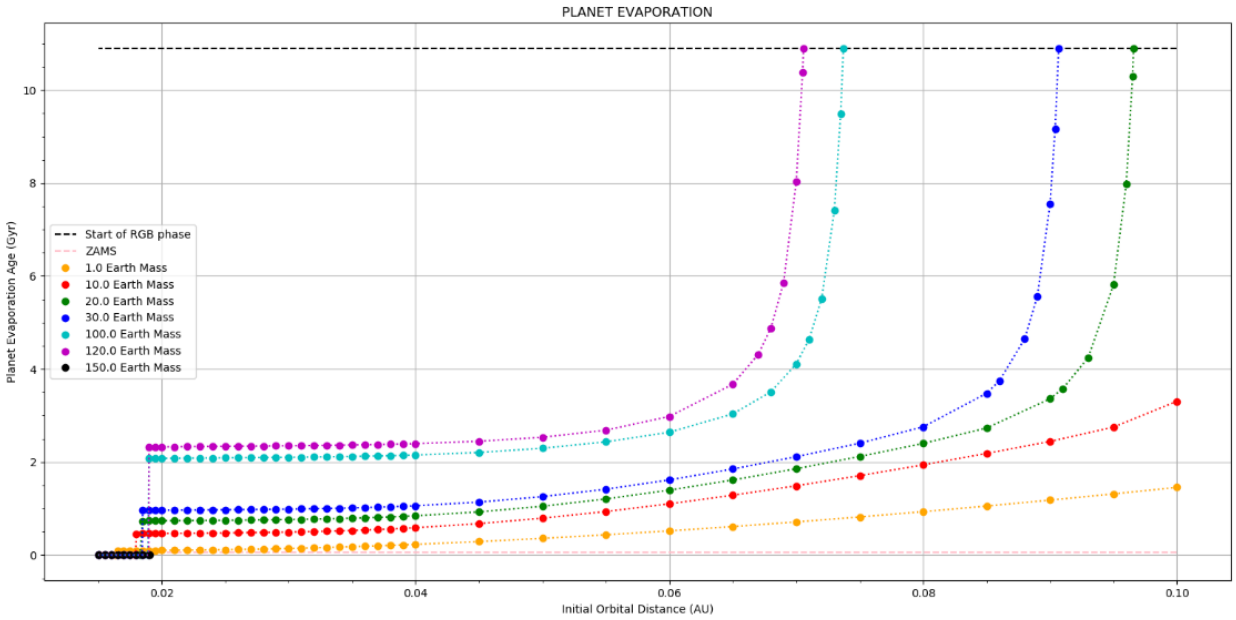

Fig. 5.1 – Time taken by planets of different masses for complete evaporation, as a function of the initial orbital distance.

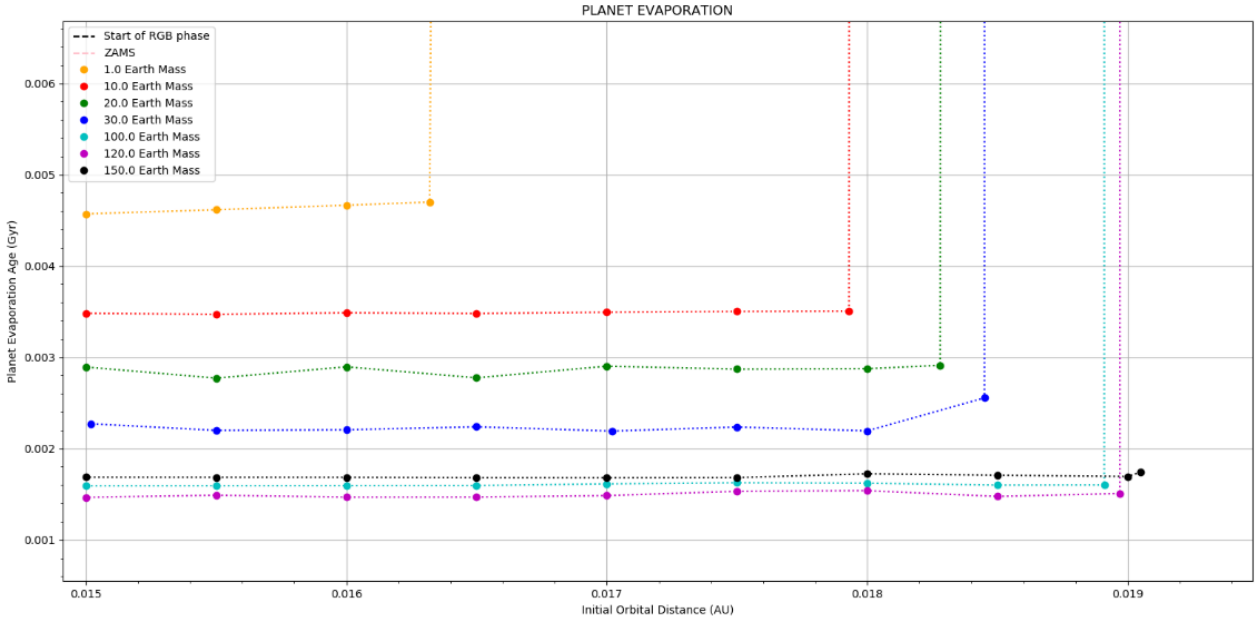

Fig. 5.2 – Zoom-in on the bottom-left part of Fig. 5.1

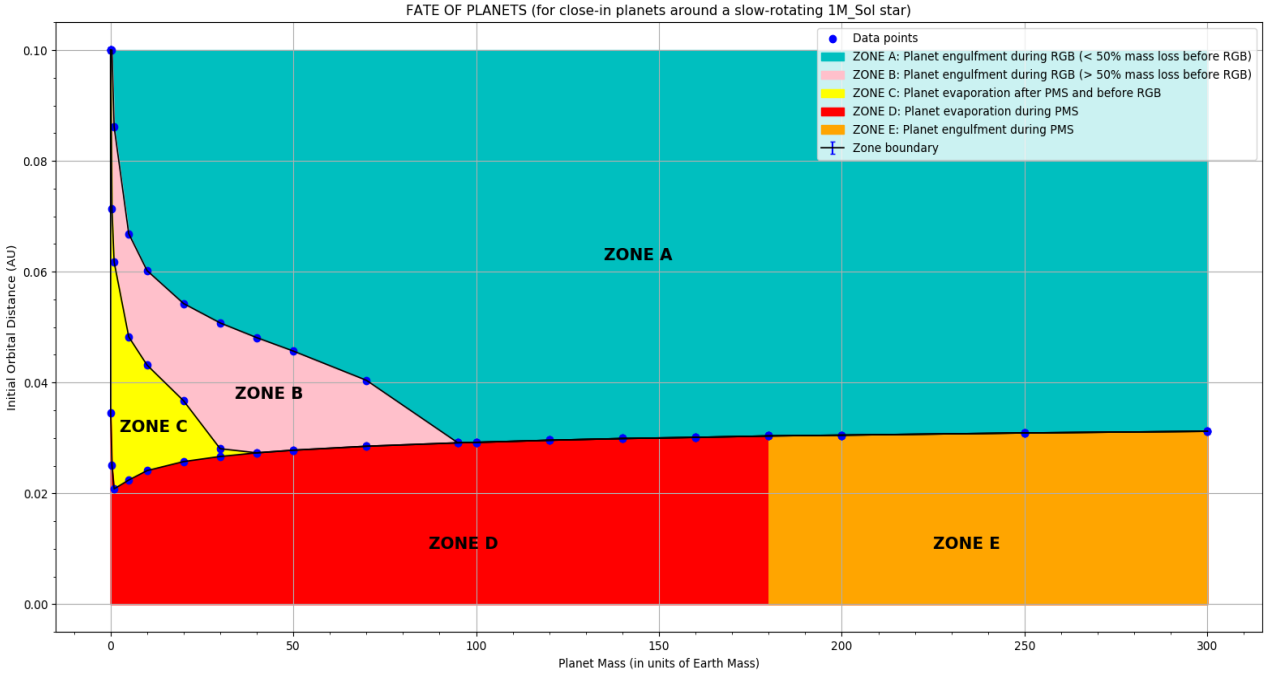

Fig. 6.1 – Fate of close-in planets around a slow-rotating 1M_Sol star

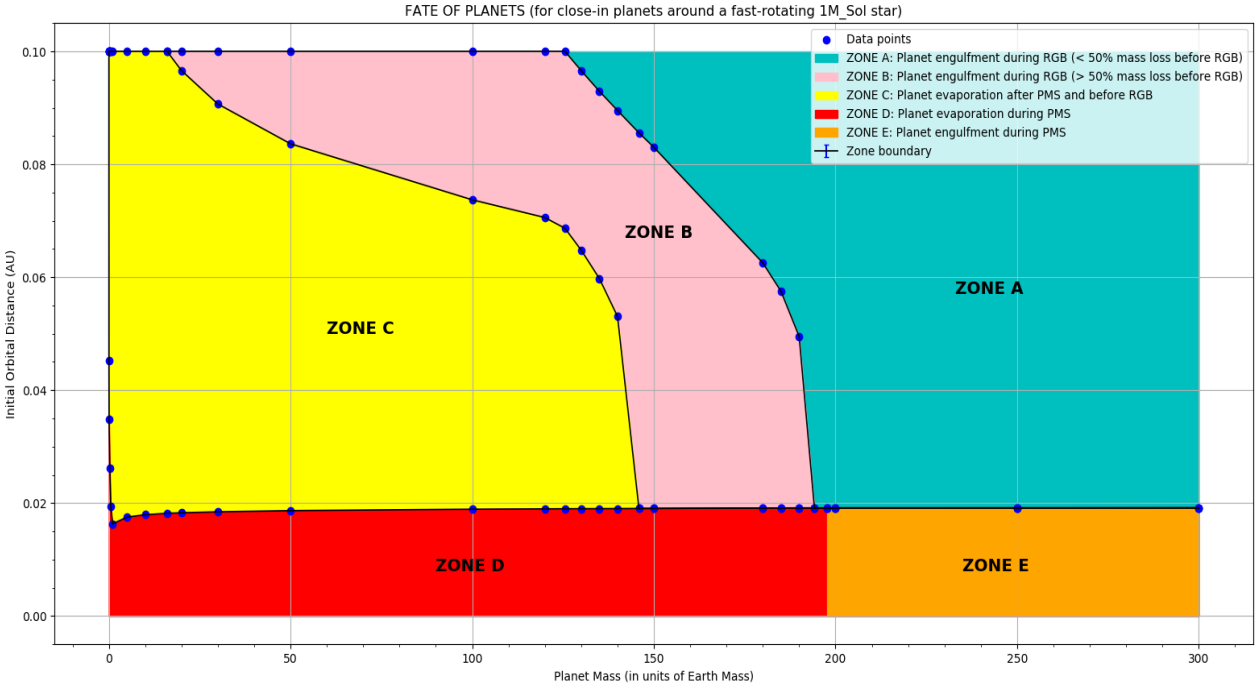

Fig. 6.2 – Fate of close-in planets around a fast-rotating 1M_Sol star

V. DISCUSSIONS AND CONCLUSIONS

- Fast rotators are those stars whose initial surface velocity is a significant fraction of the critical velocity (the velocity at which the centrifugal force at the surface overcomes gravity, which can cause the star to lose mass from its surface). From Fig. 2, we can see that regardless of initial spin (slow or fast rotator), the stellar surface velocity rapidly increases from its initial value during the PMS phase when the star is contracting. It reaches a peak, and then begins to rapidly slow down because of magnetic braking due to stellar winds, whose effect increases with increasing stellar spin.
- From Fig. 3.2 and 3.3, we can see that the orbital evolution of planets during the PMS phase of the star is dominated by Dynamical Tides, agreeing with our previous results in Rao et al. (2018). The corotation radius (which itself changes with time as the system evolves) acts as a repeller (black continuous line in the figure) – the dynamical tides pull the planet towards the star if the orbital distance is smaller than the corotation radius, otherwise they push the planet away from the star if the orbital distance is greater than the corotation radius (there are no tides if the orbital distance equals the corotation radius). Since the corotation radius decreases as the star contracts during the PMS phase, some planets which initially lie below the corotation radius may later be above it (if the orbital distance shrinks slower than the corotation radius). If this happens, the planet is now repelled away from the star. This explains the V-shaped 'kicks' in some orbits. There exists a minimum initial orbital distance such that the orbital distance fails to shrink slower than the corotation radius and always remains below it. These orbits will plunge towards the star. However, all such cases are seen to converge into the same orbit (shown as a red-dashed line). This is because of the nature of dynamical tides, which are active only if $\omega_{pl} < 2\omega_{star}$. The red-dashed line is that distance where this condition changes sign. Hence, below this line, the dynamical tides switch off and the orbit stops shrinking. But an infinitesimal time-step later, the red-dashed line shrinks, and the tides re-activate, shrinking the orbit a little more. The result is that the orbital evolution follows the red-dashed line. Depending on the mass of the planet, all orbits which are trapped into the red-dashed line end in total evaporation or otherwise engulfment of the planet by its host star.
- Close-in planets (rocky or gaseous) lose mass through evaporation upon being irradiated by XUV radiation from the star. The major contribution to the stellar XUV flux comes from the non-thermal radiation emitted by the charged stellar wind particles boosted by the star's magnetic field. This effect increases with increasing spin of the star, and it saturates at some high spin (the physics behind this comes from the magnetohydrodynamics that governs the plasma flow within the star and hence, the stellar dynamo). Note that the spin of the star is coupled to the XUV flux and to the magnetic braking due to stellar winds. The flux is coupled to the planet mass-evaporation, which affects the orbital evolution, which in turn affects the star-planet interactions (tides), which change the spin of the star. Thus, all the variables are intricately coupled, and their evolution forms a complex loop. We can see from Fig.

4.1 that a planet with given initial orbital distance loses mass rapidly in the beginning (when the stellar spin, and hence XUV flux is high) and later loses mass gradually. Also, we observe that the closer a planet is to the star, the greater is the mass-evaporation rate and the total mass lost by the planet. From Fig. 4.2, we see that below a minimum initial orbital distance, the mass-evolution curves converge and they all have the same characteristic of extremely rapid mass-loss rate. These curves correspond to those orbits in the orbital evolution plot that converge into the red-dashed line which slowly plunges towards the star. Due to their proximity to the star, the XUV flux incident on these planets is extremely high, and there is also the possibility of Roche-lobe overflow (if the planet crosses the Roche limit), explaining the disproportionately high mass-loss rates. Finally, we mention that the qualitative behaviour of mass-evolution is the same for the slow and fast-rotator case, but the mass-evaporation rates and total mass-loss are always higher for the fast-rotator case because it emits a greater non-thermal XUV flux due to its high initial spin.

- From Fig. 5.1 we see that for those planets which undergo complete evaporation below a certain initial orbital distance, the time required for complete evaporation decreases if the planet is initially kept closer to the star. Comparing the curves corresponding to planets of different masses, we observe that at a given initial orbital distance, lighter planets always evaporate faster than more massive planets, which is intuitive. A discontinuity appears in all the curves below a certain initial orbital distance (bottom-left part of Fig. 5.1 of which Fig. 5.2 is a zoomed version). This corresponds to when the planet orbits start converging into the red-dashed line as explained earlier. For these cases the planet mass-evaporation is disproportionately high, and hence there is a discontinuity in the curves and the evaporation time is very less. Fig. 5.2 tells us that since all these cases converge into the same orbit, they have similar evaporation times, and the curves are nearly flat. Interestingly, in this domain, the more-massive planets evaporate faster than the lighter planets. This counter-intuitive observation is explained by the fact that more massive planets experience stronger tides and are drawn closer to the star faster than less massive planets. Hence, the net result is that even though they have more mass, the massive planets evaporate faster. However, this trend is again reversed beyond a certain mass-limit (~120*M_Earth for the fast-rotator case) when the planet has enough mass to resist evaporation even if it is closer to the star compared to lighter planets. This explains why the 150*M_Earth curve lies above the others in Fig. 5.2. Also, note that beyond a certain mass limit, the planets only evaporate completely if they enter the converging orbit. That is why the 150*M_Earth curve exists only in the lower-bottom part of Fig. 5.1. Although these plots show the cases for a fast-rotating 1M_Sol star, the results for a slow-rotator will be qualitatively similar.
- *Figures 6.1 and 6.2 are the most impactful plots of all and provide a complete picture of the study.* For the slow and fast-rotating 1M_Sol star cases respectively, these plots show the various fates that close-in planets can suffer depending on their initial mass and orbital distance. Running the star-planet evolution code for several combinations of initial planet mass and orbital distance in our selected domain and analysing the data allows us to classify the planet fates into 5 types, seen in the plots as 5 different

coloured zones. Planets which start off in Zone A lose less than 50% of their total mass due to evaporation by the start of the RGB phase, but they get engulfed by the star during the RGB phase. Planets beginning in Zone B suffer a similar fate, but they lose >50% of their total mass by the start of the RGB phase. Planets beginning in Zone C suffer complete evaporation sometime during the MS phase. Zones D and E correspond to those cases whose orbits converge into the red-dashed line as explained earlier. In this region, less massive planets always completely evaporate during the PMS phase. There exists a mass-limit (which depends on the initial spin of the star), above which the planet has enough mass to resist complete evaporation but gets engulfed by the star instead (also during the PMS phase). This causes Zone D to transition into Zone E. It is interesting to note that a planet of given mass can suffer a variety of different fates at different initial orbital distances. For instance, a 140*M_Earth planet could be in Zone A, B, C or D depending on the initial orbital distance. We observe that massive planets (hot-Jupiters) exclusively suffer engulfment (either during the PMS or the RGB) and never fully evaporate, while lighter planets can suffer a variety of fates depending on the initial mass and orbital distance. It is also interesting to note that there exist several mass-limits (the 'triple-points' on the plots) beyond which some fates become inaccessible to the planet at any initial orbital distance. On the other hand, there exist other mass-limits beyond which new fates become accessible to the planet at the appropriate initial distances. Finally, we compare how the planet fate diagram changes as we go from a slow-rotating to a fast-rotating star. We note that fast-rotators are deadlier for planets because they have stronger tides and a higher XUV flux. Going from a slow to a fast rotator, the sizes of Zones D and E reduce slightly because fast-rotators have a smaller corotation radius. But Zones B and C are greatly expanded at the expense of Zone A because planet mass-evaporation rates are higher for a fast-rotator case. Finally, we note that the results agree with the observations that we are more likely to observe hot-Jupiters close to the host star (Zone A) than small rocky planets (Zone C), which completely evaporate during the MS phase.

VII. REFERENCES

1. *Rao et al. (2018) and all references therein:* https://arxiv.org/abs/1807.01474
2. *MacGregor, K. B. & Brenner, M. 1991, ApJ, 376, 204*
3. *Allain, S. 1998, A&A, 333, 629*
4. *Matt S. P., MacGregor K. B., Pinsonneault M. H., Greene T. P., 2012, ApJ, 754, L26*
5. *See V., et al., 2017, MNRAS, 466, 1542*
6. *Parker (1958): ApJ, vol. 128, p.664*
7. *Bashi, Helled, Zucker and Mordasini (2017) : A&A 604, A83 (2017)*
8. *Bondi & Hoyle (1944) : MNRAS, Vol. 104, p.273*
9. *Lalitha et al. (2018) and all references therein: MNRAS 477, 808–815 (2018)*
10. *Tu, Johnstone, Güdel, and Lammer (2015): A&A 577, L3 (2015)*
11. *Spada, F., Lanzafame, A. C., Lanza, A. F., Messina, S., & Collier Cameron, A. 2011, MNRAS, 416, 447*